Velocity analysis and imaging in transversely isotropic media:

Methodology and a case study

TARIQ ALKHALIFAH, ILYA TSVANKIN, KEN LARNER
Colorodo School of Mines
Golden, Colorado

JOHN TOLDI
Chevron Overseas Petroleum
San Ramon, California

Physicists and mathematicians, for many years, have studied the intricacies and complexities of how elastic waves propagate in anisotropic media (media in which velocity varies with direction of propagation). Moveover, over the years, a select few visionary exploration geophysicists (e.g., G. Postma, F. Levin, and K. Helbig) have been telling us that the earth's subsurface is not isotropic, so processing that fails to take anisotropy into account should yield biased estimates of depth and subsurface velocity. Nevertheless, it is only in this past decade that the anisotropic character of the earth's subsurface has been seriously studied and treated. During that time, most emphasis has been focused on the influence of anisotropy on the behavior of shear waves (e.g. Crampin 1985, a common belief being that departures of medium properties from isotropic waves were of second order for *P-waves.*

This is understandable since if one does not look for the existence of anisotropy in *P-wave* data, it can often go unnoticed. That being the case, what then is the issue with ignoring its presence? Simply, where the subsurface is anisotropic, and evidence increasingly suggests that anisotropy is rather pervasive, processing that makes the erroneous assumption of isotropy yields errors in seismic images and, thus, interpretations. One of the anisotropy-related phenomena that was recognized more than a decade ago is that of misties in time-to-depth conversion caused by the difference between the stacking and vertical velocity in anisotropic media. Also recently attracting the attention of the exploration community are the difficulties experienced by conventional processing methods (i.e., those based on the assumption of isotropy) in imaging of dipping reflectors, such as fault planes, below transversely isotropic formations.

The case study described here represents a dramatic example of the inadequacy of conventional imaging methods in the presence of seismic anisotropy. Figure I shows a seismic line from offshore Africa acquired by Chevron Overseas Petroleum. The line was processed using a sequence of conventional normal moveout, dip moveout, and poststack time migration algorithms without taking anisotropy into account. While horizontal and mildly dipping reflectors look sufficiently sharp, steep fault planes (such as the one at 1.5-2 s to the left of CMP 1000, dipping at about 40°) are poorly focused and imaged.

To find the cause of the problem, it is useful to examine the constant-velocity stacks (CMP stacks generated at certain constant values of the stacking velocity) after application of conventional constant-velocity DMO (Figure 2). The goal of DMO processing is to focus both horizontal and dipping events on the same velocity panel. However, while subhorizontal reflectors at times between 1.5 and 2 s are imaged best at a stacking velocity of 2200 m/s, the steep reflection comes into focus at a much higher velocity (2400-2450 m/s). As a result, the conventional processing sequence produces a weak, blurry image of the dipping fault plane. We note that the dip of the fault plane is not uncommonly large (about 40°).

If the DMO problem had been caused by a velocity gradient in an *isotropic* medium, we would expect the dipping event to be imaged at a lower stacking velocity than that of the horizontal event, just the opposite of what we see in Figure 2. We suggest, instead, that the DMO algorithm fails to remove the dip-dependence of stacking velocity as a result of the increase in the stacking velocity for reflections from dipping interfaces caused by anisotropy. Below, we demonstrate that this problem can be corrected by properly accounting for anisotropy in DMO processing.

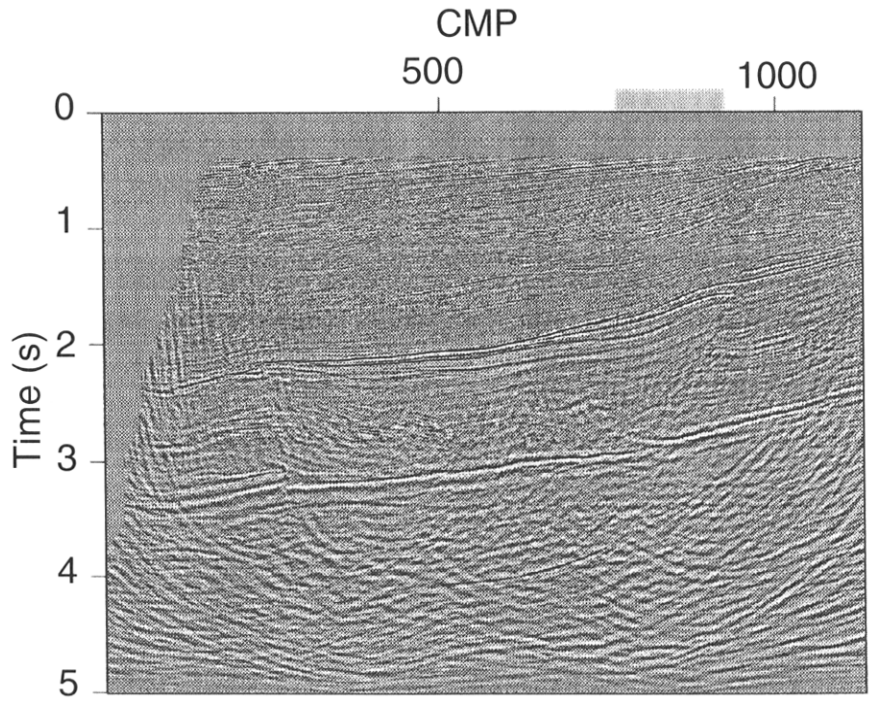

Figure 1. Time-migrated seismic line (offshore Africa). The gray bar to the left of CMP 1000 shows the range of CMP locations examined in Figures 2 and 7.

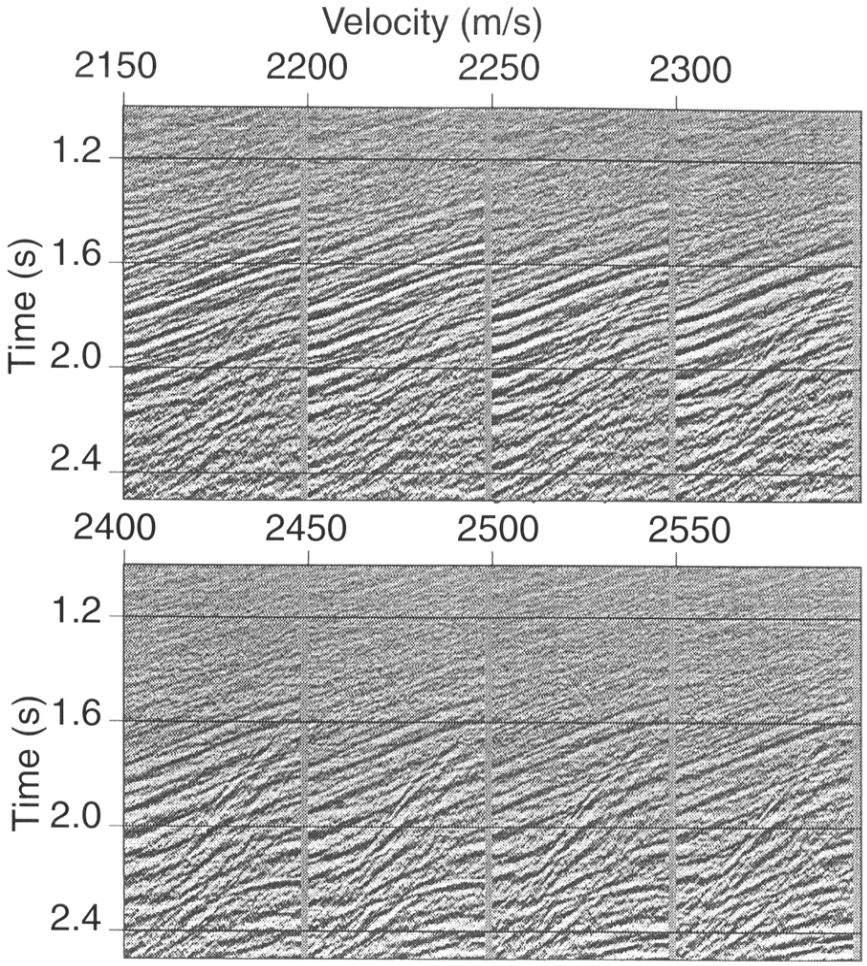

Figure 2. Constant-velocity stacks after the conventional NMO-DMO sequence (without accounting for anisotropy). The velocity values at the top correspond to the stacking velocity used in the NMO correction. The mildly dipping events (e.g., those at times of 1.5-1.8s) will he called "subhorizontal" in the text.

As mentioned above, anisotropy also often manifests itself through misties in time-to-depth conversion. Although the imaging issues (i.e., DMO and time migration) are the primary subject of this paper, a brief look at time-to-depth conversion shows evidence of large anisotropy and provides some insight into the geologic section responsible for the anisotropic phenomena. Figure 3 presents this evidence in the form of a comparison between average velocities derived from check shots and those derived from reflection moveout in surface seismic data. Note that the separation of the two curves continues to increase down to about 2 s two-way time, then remains constant for the remainder of the measurements. The maximum separation amounts to a 12% mis-tie in the average velocity; similar sizable misties have been observed by Ball (1995) in an adjacent area and attributed to the influence of anisotropy. Below, we interpret the mis-ties in terms of Thomsen's (1986) anisotropy parameter δ.

Once the importance of anisotropy is accepted, two further impediments to taking its presence into account must be overcome: (I) processing algorithms that include anisotropy are more complex than those that ignore it, and (2) even with such processing capability at hand, heretofore it has been difficult to estimate the anisotropy parameters required by these algorithms. The second problem has seemed to be especially intimidating. It has been believed that estimation of the four or more parameters that fully characterize P-wave propagation in typical anisotropic media is not only difficult (estimating the one critical parameter for isotropic media - velocity - is difficult enough), the task also seemed to require additional measurements beyond those obtained in conventional seismic surveys (e.g., crosswell, vertical seismic profiles, or auxiliary S-wave data). For instance, conventional velocity analysis based on short-spread moveout (stacking) velocities does not provide enough information to determine the true vertical velocity in transversely isotropic media with a vertical symmetry axis (VTI media). (Velocity in VTI media varies with direction of propagation away from the vertical. but not with azimuth.)

It turns out, however, that it is *not necessary* to know the vertical velocity for anisotropic *time* processing. The influence of vertical transverse isotropy on NMO, DMO, and time migration is governed by the short-spread NMO (stacking) velocity from horizontal reflectors (determined by conventional velocity analysis) and a single anisotropic parameter (we denote it as η) that can be obtained from the dip-dependence of *P-wave* NMO velocity. After a brief description of our approach to parameter estimation, we return to the field-data example to demonstrate significant improvements in structural imaging achieved by the new anisotropic processing sequence.

Anisotropy parameters and velocity analysis of P-wave data. Throughout this paper we consider the most common anisotropic model — VTI media - but we do not assume that anisotropy is weak or elliptical. Both assumptions are inappropriate for shales. which represent the most common source of transverse isotropy in sedimentary basins. Conventionally, *P-wave* (strictly, *quasi-P-wave)* and *SV-wave (quasi-SV-wave)* propagation in Tl media have been described by four stiffness coefficients c_{ij}. Recognizing value in combining these stiffness coefficients to form four alternative anisotropy parameters that likewise characterize TI media, Thomsen (1986) defined four anisotropy parameters: V_{P0} (the *P-wave* velocity in the direction of the symmetry axis), V_{S0} (the S-wave velocity in the same direction), ϵ (a dimensionless quantity close to the fractional difference between the velocities in the directions perpendicular to and parallel to the symmetry axis), and δ (another dimensionless quantity that predominantly governs the variation of *P-wave* velocity close to the symmetry direction, which is vertical for VTI media). Measured values of the ratio of horizontal to vertical velocity (an often quoted measure of anisotropy) in some sedimentary basins can be 1.3 and larger. As it happens, however, this parameter, ϵ, *has no direct influence* on most seismic data processing.

Although Thomsen found this new

notation to be particularly convenient for developing analytic expressions for wave behavior under the assumption of "weak anisotropy" (i.e., $|\epsilon| << 1$ and $|\delta| << 1$), the fully comprehensive value of these parameters has since emerged for media with *any degree* of anisotropy. For example, Tsvankin and Thomsen (1994) found that the kinematics of *P-wave* propagation are, for practical purposes, independent of one of these parameters - V_{S0}. Likewise, seismic signatures of importance in reflection seismology, such as normal moveout velocities, take a relatively simple form if expressed through Thomsen parameters. For example, the *P-wave* normal moveout velocity (the stacking velocity in the limit of small offset) in a single horizontal VTI layer is given by

$$V_{nmo}(\phi = 0) = V_{P0}(1 + 2\delta)^{1/2} \quad (1)$$

where ϕ is the reflector dip. The relation between the NMO velocity and dip is discussed below. We would like to emphasize that this equation is valid for any strength of the anisotropy. For a more detailed discussion of notation, see Tsvankin (1996).

In layered VTI media, NMO velocity is equal to therms average of the interval NMO values given by equation (1). Hence, the parameter δ is responsible for the difference between the true (rms) vertical velocity and NMO (stacking) velocity in VTI media. as exemplified for our study area in Figure 3. By recasting the two sets of measurements in Figure 3 in terms of interval velocity, we derived the δ curve shown in Figure 4. The value of δ reaches a surprisingly large value of .4 at 2.2 s, then rapidly drops almost to zero. The overall shape of this δ curve correlates well with our understanding of the geologic section. The Tertiary section (everything above the strong reflector located at about 2.3 s below CMP 200 in Figure 1) is known to be predominantly shale; between this reflector and the basal detachment (the bright reflector at ***3.2*** s), the Cretaceous section is a complex mixture of sands, shales, and carbonates. Evidently, the Tertiary shales are primarily responsible for this large anisotropy, and indeed become increasingly anisotropic with depth.

In the example above, we have used borehole measurements (check shots) to recover 6. From surface seismic data alone, it is impossible to separate V_{P0} and δ even by recording the conventional spread moveout of the *SV-wave* in addition to that of the *P-wave;* NMO velocity remains the only parameter that can be extracted using moveout data from horizontal reflectors.

The presence of structure at depth and generation of reflections from dipping planes, however, provide new information for anisotropic inversion by extending the angle coverage of surface data. If the medium above the reflector is anisotropic but homogeneous, the dip-dependence of NMO velocity for any pure mode (e.g., *P-P, SV-SV)* can be represented as a relatively simple function of phase velocity and its derivatives taken at the dip ϕ (Tsvankin, 1995):

$$V_{\mathrm{nmo}}(\phi) = \frac{V(\phi)}{\cos\phi} \frac{\sqrt{1 + \dfrac{1}{V(\phi)} \dfrac{d^2V}{d\theta^2}\Big|_{\theta=\phi}}}{1 - \dfrac{\tan\phi}{V(\phi)} \dfrac{dV}{d\theta}\Big|_{\theta=\phi}}, \quad (2)$$

where V is the phase velocity, that is, the velocity of a plane wave propagating at angle θ measured from vertical. The only assumption about anisotropy underlying the anisotropic NMO equation given just above is that the incidence (sagittal) plane is a plane of symmetry of the medium (it should also be in the dip plane of the reflector).

If the medium is isotropic, the derivatives of phase velocity with respect to direction vanish, and this equation reduces to the familiar cosine-of-dip dependence

$$V_{nmo}(\phi) = \frac{V}{\cos\phi};$$

We see, therefore, that the directional dependence of velocity [i.e., the derivatives in the equation(2)] in VTI media give rise to departures from the "isotropic" behavior of NMO velocity. It is these departures that we will use for parameter estimation in VTI media.

Although equation (2) was derived in the zero-spread limit, it accurately describes *P-wave* moveout for conventional spread lengths, i.e., those comparable to the distance between the CMP and the reflector. For purposes of seismic processing, NMO velocity is more conveniently represented as a function of the ray parameter $p(\phi)$, which is just the slope of reflections observed on zero-offset (or CMP-stacked) seismic sections. As shown by Alkhalifah and Tsvankin (1995). *P-wave* NMO velocity for reflections from dipping planes [equation(2)] as a function of *p* is determined by just *two* parameters: the NMO velocity from a horizontal reflector [equation(l)] and a dimensionless combination of the Thomsen parameters given by

$$\eta \equiv \frac{\epsilon - \delta}{1 + 2\delta}.$$

In the limit of weak anisotropy (i.e., small parameters ϵ and δ), η reduces to

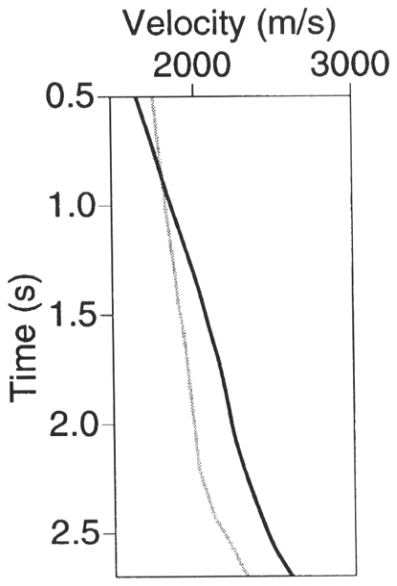

Figure 3. Average P-wave vertical velocity from check-shot data (gray curve) and stacking velocity from surface seismic data converted into average velocity (black curve), both as functions of vertical time. The measurements are taken near CMP 200 in Figure 1.

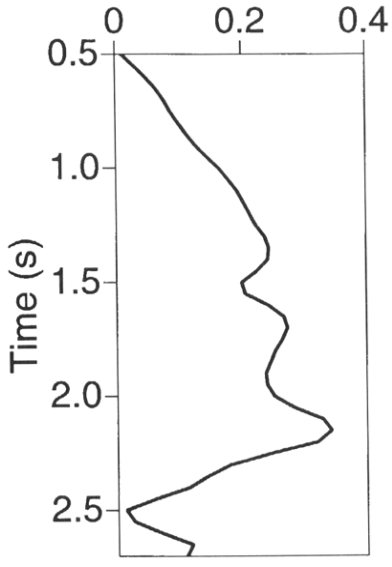

Figure 4. The parameter δ obtained from the velocity curves in Figure 3. The measurements are taken near CMP 200 in Figure 1.

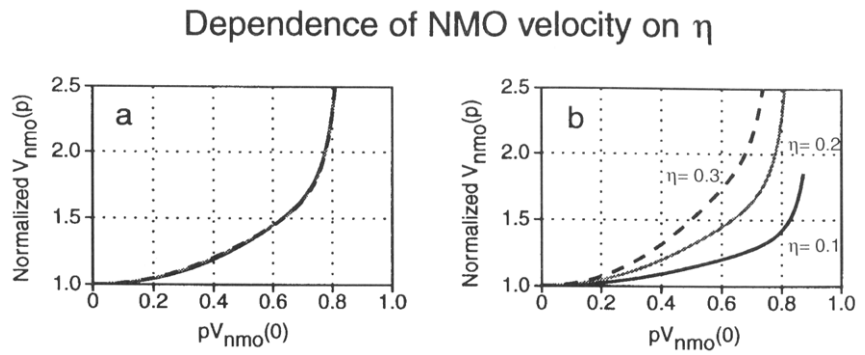

Figure 5. P-wave normal moveout velocity from dipping reflectors normalized by the conventional NMO expression for isotropic media. If the medium were isotropic, the normalized NMO velocity would equal unity for all values of slope p. The dips for these values of $pV_{nmo}(0)$ range from 0 to 70°. (a) Three very different models with the same η= 0.2: ϵ = 0.1, δ = -0.071 (solid black); ϵ = 0.2, = 0 (gray); ϵ = 0.3, δ = 0.071 (dashed) - the curves practically coincide. (b) models with three different values of η: η = 0.1 (solid black); η = 0.2 (gray); η = 0.3 (dashed).

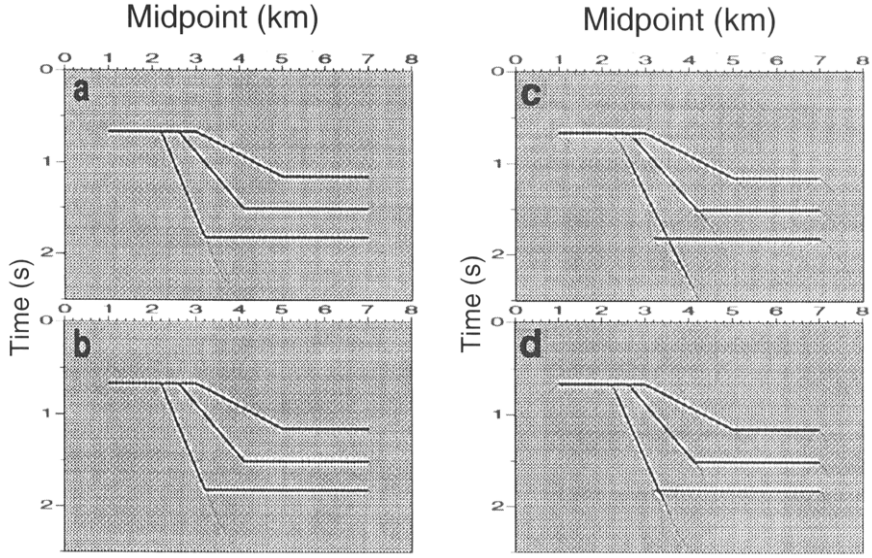

Figure 6. Anisotropic time migrations of zero-offset synthetic data generated by ray tracing. The model parameters are V_{P0} = 3.0 km/s, ϵ = 0.2 and δ = 0.1 (i.e., $V_{nmo}(0)$ = 3.29 km/s, η = 0.0833). The sections on the left were obtained using the actual model (a); a very different model (V_{P0} = 2.6 km/s, ϵ = 0.433 and δ = 0.3) that still has the correct values of $V_{nmo}(0)$ and η (b). On the right, the models have the correct value of $V_{nmo}(0)$ but the wrong value of η: η = 0.01 (c) and η = 0.06 (d).

the difference ϵ-δ. Note that the coeffcient η goes to zero not only for isotropic media (ϵ=δ=0), but also for any elliptically anisotropic media (i.e., media for which ϵ =δ). Thus, the dependence of the NMO velocity on the ray parameter for isotropic media holds for elliptical models as well, but becomes inadequate for general transverse isotropy.

Figure 5a shows that the P-wave NMO velocity as a function of the ray parameter of dipping events ("dip-moveout signature") is controlled solely by η and does not depend on the individual values of the anisotropy parameters ϵ and δ. For most typical media, η > 0 (that is, ϵ > 0). the conventional DMO expression based on the cosine-of-dip equation severely understates NMO velocities for dipping reflectors. This implies that conventional constant-velocity DMO designed for isotropic media breaks down in the presence of transverse isotropy (recall the field-data example in Figure 2).

To obtain the parameters $V_{nmo}(0)$ and η using the second equation, it is sufficient to have *P-wave* NMO velocities and ray parameters measured for two distinctly different dips. If one of the reflectors is horizontal (a common situation), then $V_{nmo}(0)$ is obtained by conventional velocity (e.g., semblance) analysis, and the parameter η remains the only unknown to be recovered. This inversion procedure is stable in that the inverted values of the parameters $V_{nmo}(0)$ and η are not too sensitive to errors in the input NMO velocities. Indeed, the spread of curves in Figure 5b suggests that the NMO-velocity curves corresponding to values of η = 0.1,0.2, and 0.3 are well resolved over a wide range of dips. Alternatively, η can be constrained, albeit with a lower accuracy, using nonhyperbolic moveout on long spreads.

Once the parameters $V_{nmo}(0)$ and η have been determined, the normal moveout velocity can be computed for any value of the ray parameter. This algorithm makes it possible to carry out anisotropic dip-moveout corrections without using any information other than *P-wave* reflection moveout. Moreover, Alkhalifah and Tsvankin showed that not just DMO, but also *all* time-related imaging steps (i.e., NMO, DMO, and poststack and prestack time migration) depend on the same two parameters. The parameter η is also responsible for anisotropy-induced nonhyperbolic moveout, which may distort the stack of data from relatively long spreads (where the spread length-&-depth ratio is on the order of 1.5-2). The fact that time processing is controlled by just two parameters (instead of four), one of which (V_{nmo}) is routinely determined by conventional velocity analysis, is an extremely important result that makes anisotropic imaging a practical endeavor.

Figure 6 shows anisotropic prestack Gazdag time migrations of synthetic zero-offset data generated for a structural model embedded in a homogeneous VTI medium. The image in Figure ha was obtained using the actual model parameters in the migration, while Figure 6b was obtained by migrating using a model with different values of V_{P0}, ϵ, and δ, but with the *same* $V_{P0}(0)$ and η. Although the model used for the migration result in Figure 6b has anisotropy parameters that differ substantially from those of the actual one, it has the correct values of $V_{nmo}(0)$ and η and, consequently, produces an accurate image.

The two images in Figures 6c and 6d show migrated sections generated using inaccurate values of η. The errors, apparent in both cases, demonstrate the sensitivity of the migration results to the value of η. Predictably, the distortions are more pronounced for the model with a larger error in η: not only do the imaged reflectors cross but also the re-

Table 1. f-wave parameters for vertical transverse isotropy in Thomsen notation

Full set	Velocities, depth imaging	Time imaging	AVO (intercept, gradient)
V_{P0}	V_{P0}	$V_{nmo}(0)$	V_{P0}
ε or η	ε or η	η	—
δ	δ	—	δ
V_{S0}	—	—	V_{S0}

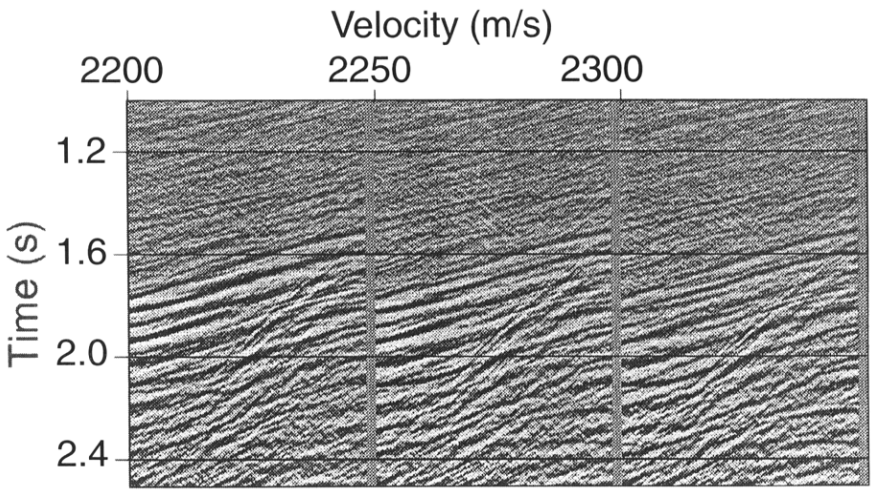

Figure 7. Constant-velocity stacks of the offshore Africa data after the NMO-DMO sequence adapted for homogenous VTI media. The velocity values at the top correspond to the stacking velocity for subhorizontal reflectors and η = 0.07.

flector edges are not imaged well. Hence, errors in the parameters V,,,(O) and η lead to distortions in the migrated images that can be used to refine the inversion results.

While NMO, DMO, and time migrations in VTI media have been made practical by the wonderfully simple result that the kinematics and thus all time-related imaging depend on just two parameters, both of which are accessible from conventional surface seismic data, other information (e.g., check shots or *SV-wave* moveout) is still required in order to make the all-important conversion from time to depth. Table 1 offers a reference guide that shows the sets of parameters required for time and depth P-wave imaging, as well as amplitude variation with offset analysis in VTI media. If the parameters $V_{nmo(}0)$ and η have been obtained but the vertical velocity is unknown, the image produced by the sequence of NMO, DMO, and poststack *depth* migration will be well-focused but may have the wrong depth scale. Note that knowledge of η is insufficient for performing anisotropic AVO analysis because the gradient AVO term depends on the values of δ and V_{S0}.

Anisotropic processing of an offshore data set. The field data introduced in Figure 1 come from a part of West Africa in which seismic anisotropy has been recognized to be significant. As we have discussed above, the anisotropy manifests itself both in time-related imaging and in time-to-depth conversion. In the section displayed in Figure 1, the gentle dips are well imaged by conventional methods. However, improved imaging of the more steep fault-plane reflections would significantly aid the interpretation of this data set. A clear picture of the faulting in the Cretaceous sections is an essential component of our understanding the extent of the oil fields in this area. Below we demonstrate that dramatic improvement in the imaging of dipping reflectors can be achieved by taking anisotropy into account.

First, we show that the dipping event missed by conventional DMO in Figure. 1 can be properly focused by an anisotropic DMO algorithm. We have picked the best-tit stacking velocities and the corresponding ray parameters for the subhorizontal and dipping events from constant-velocity stacks (Figure 2) and applied our inversion algorithm, assuming a homogeneous VTI medium above the dipping reflector. The inversion procedure yielded the value of η = 0.07, which was used to reprocess the data by means of a TZO (transformation to zero offset) ray-tracing algorithm designed for VTI models (Alkhalifah, 1996). As seen in Figure 7, the anisotropic TZO succeeded in focusing both the subhorizontal and dipping events on the same velocity panel -the one corresponding to the best-fit stacking velocity (V_{stack}=2250 m/s) for the subhorizontal reflectors.

The anisotropic processing sequence described above is based on the assumption that the medium above the dipping reflector is homogeneous. However, analysis of the time dependence of the zero-dip stacking velocity, which can be approximated by V.,,,(O), shows a pronounced velocity gradient of about 0.7 s^{-1} in this study area. Therefore, the coefficient η produced by the inversion algorithm should be regarded as an "effective" parameter that reflects the combined influence of anisotropy and inhomogeneity. To account for vertical inhomogeneity in time-related processing, it is necessay to recover parameters $V_{nmo}(0)$ and η as functions of the vertical reflection time. The time dependence of the zero-dip NMO velocity $V_{nmo}(0)$ can be obtained through semblance analysis of reflections from subhorizontal interfaces and subsequent Dix differentiation as is done for isotropic media. To determine the parameter η in vertically inhomogeneous media, we use the Dix-type equation for dipping reflections given by Alkhalifah and Tsvankin. Their equation is a generalization of the conventional Dix formula in that all velocities and traveltimes are evaluated at the ray-parameter value corresponding to the dip of the reflector. For nonelliptical VTI media, application of the generalized Dix equation requires the presence of a through-going dipping reflector (or several dipping reflectors) in all layers.

Figure 8 shows another migrated seismic section from the same general area, offshore Africa. This section, commercially processed, exhibits more complicated subsurface structure with reflections from a large number of dipping fault planes. The upper layers (above 3.0 s at CMP 750 and above 2.1 s at CMP 1050) are largely composed of

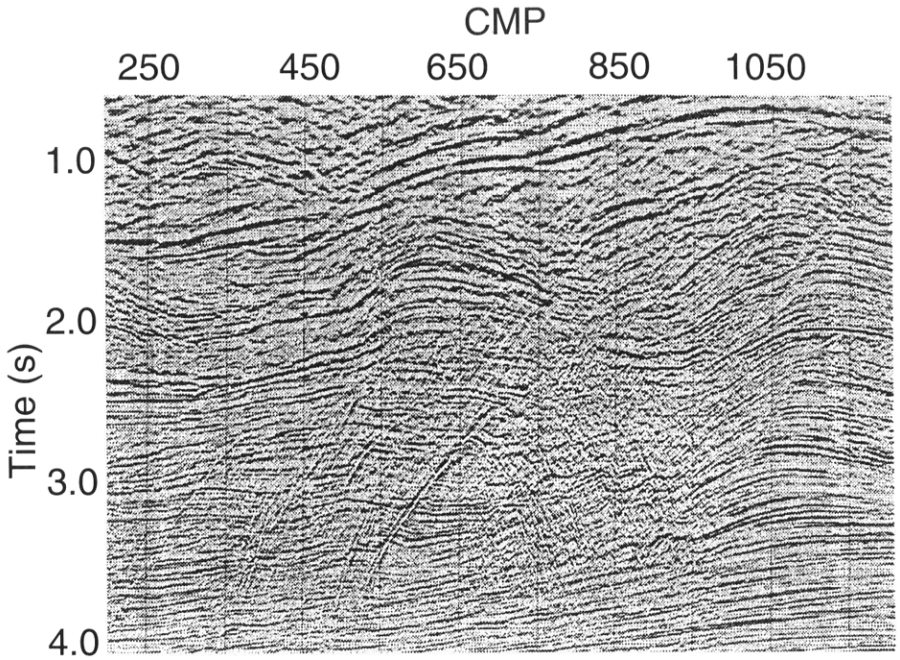

Figure 8. Time-migrated section based on 3-D isotropic processing.

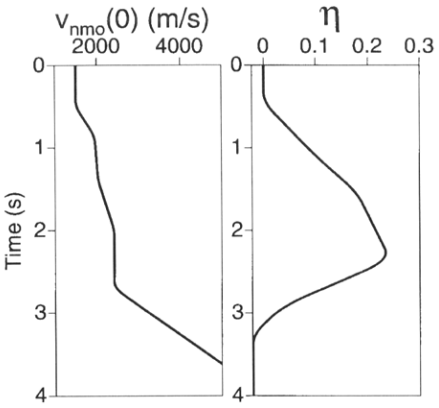

Figure 9. Interval values of V.,.(O) and η as functions of the vertical time estimated from reflections over the CMP range 600-850.

high-pressure shales that are believed to be the main source of the anisotropy in the data.

The line in Figure 8 is the output of a conventional 3-D processing sequence based largely on the assumption of isotropy. The only exception was use of a "stretched" DMO algorithm designed to compensate empirically for the influence of anisotropy on the dip-dependent NMO velocity and DMO impulse response. The stretched DMO, however, can provide only an approximation of the actual DMO signature in VTI media (Alkhalifah, 1996); therefore, its use was met with only partial success in this complicated area.

The inversion process based on the generalized Dix equation and a piecewise-linear assumption about $V_{nmo}(0)$ and η yielded the time dependence of the parameters $V_{nmo}(0)$ and η shown in Figure9 (Alkhalifah, 1995). Smoothing was used to remove the sharp edges that arise at times where stacking velocity was measured. In the water layer, $V_{nmo}(0)$= 1.5 km/s and, obviously, η = 0. Down to about 2.5 s, the interval values of η in Figure 9 show an increase with vertical time. At times exceeding 3.5 s, we had no adequate dip moveout information on η. As in conventional velocity analysis, further refinement of the spatial distribution of η can be achieved through migration velocity analysis, which can be based, for instance, on a depth-focusing approach.

Although the δ curve in Figure 4 does not correspond to the same CMP location as does the η curve in Figure 9, it is interesting that the overall shape of the δ and η curves is similar. Note that both anisotropic parameters are positive in the Tertiary shale section, with particularly large values near the bottom of the shale formation. Potentially, this correlation between the anisotropic coefficients can be used in time-to-depth conversion. Indeed, while time imaging requires knowledge just of the coefficient η, the vertical velocity (or δ) is the key parameter needed to obtain a depth image. Surface P-wave seismic data alone are not sufficient to recover the true vertical velocity. In the early phase of field development, velocity information from surface seismic measurements usually is combined with the initially sparse well control to determine the depth structure away from a crestal position. This combination has typically been based on spatial interpolation of the mis-tie values. With a moderate degree of correlation between the δ values computed at the wells and nearby η values extracted from the seismic data, we have the intriguing possibility of using η measurements away from the wells to help us predict δ, and thus the time-to-depth relationships at those locations.

Figure I Oa shows the output of a convention isotropic (but this time 2-D) processing sequence that included constant-velocity DMO and phase-shift time migration. For comparison, Figure 10b shows the 2-D data imaged with phase-shift VTI time migration (using the inverted parameters of Figure 9) applied to the stacked section obtained by a DMO algorithm devised for vertically homogeneous VTI media. This comparison gives a clear picture of the benefits of taking anisotropy into account in seismic imaging; the improvements here are numerous and significant. Probably the most dramatic example is the fault located at CMP 870 between 2.5 and 3 s. An interpreter using the isotropic-processing result might readily either extend the reflections across this fault (invisible on the isotropic section) or suggest a minor subsidence to the left of the fault. The anisotropic image and the inverted interval values of η, however, suggest that shales extend all the way down to 3 s under CMP 800. thus indicating a much larger subsidence.

The anisotropic section also shows a significant improvement in the continuity of the dominant fault plane that extends from under CMP 900 (a time of about I s) all the way down to 3 s beneath CMP 500. Another example is the region of the nearly horizontal events near CMP location 500 at 2.5 s. The improved continuity of the gently dipping events likely is a result of the nonhyperbolic moveout correction included in the anisotropic processing sequence.

It should be emphasized that the 2-D anisotropic processing result (Figure 10b) shows a significant improvement in focusing the dipping events over the 3-D isotropic migrated section in Figure 8. This, of course, is not to say that 2-D anisotropic processing produces a better image of the subsurface than does 3-D isotropic processing. Treating just anisotropy or three dimensionality alone is necessarily incomplete. Where the subsurface has even modest three-dimensional complexity, it is best to incorporate the VTI algorithms into 3-D processing, a worthy goal for future work.

The fault reflections above 2 s in Figure 8 were accurately positioned despite the presence of anisotropy. Per-

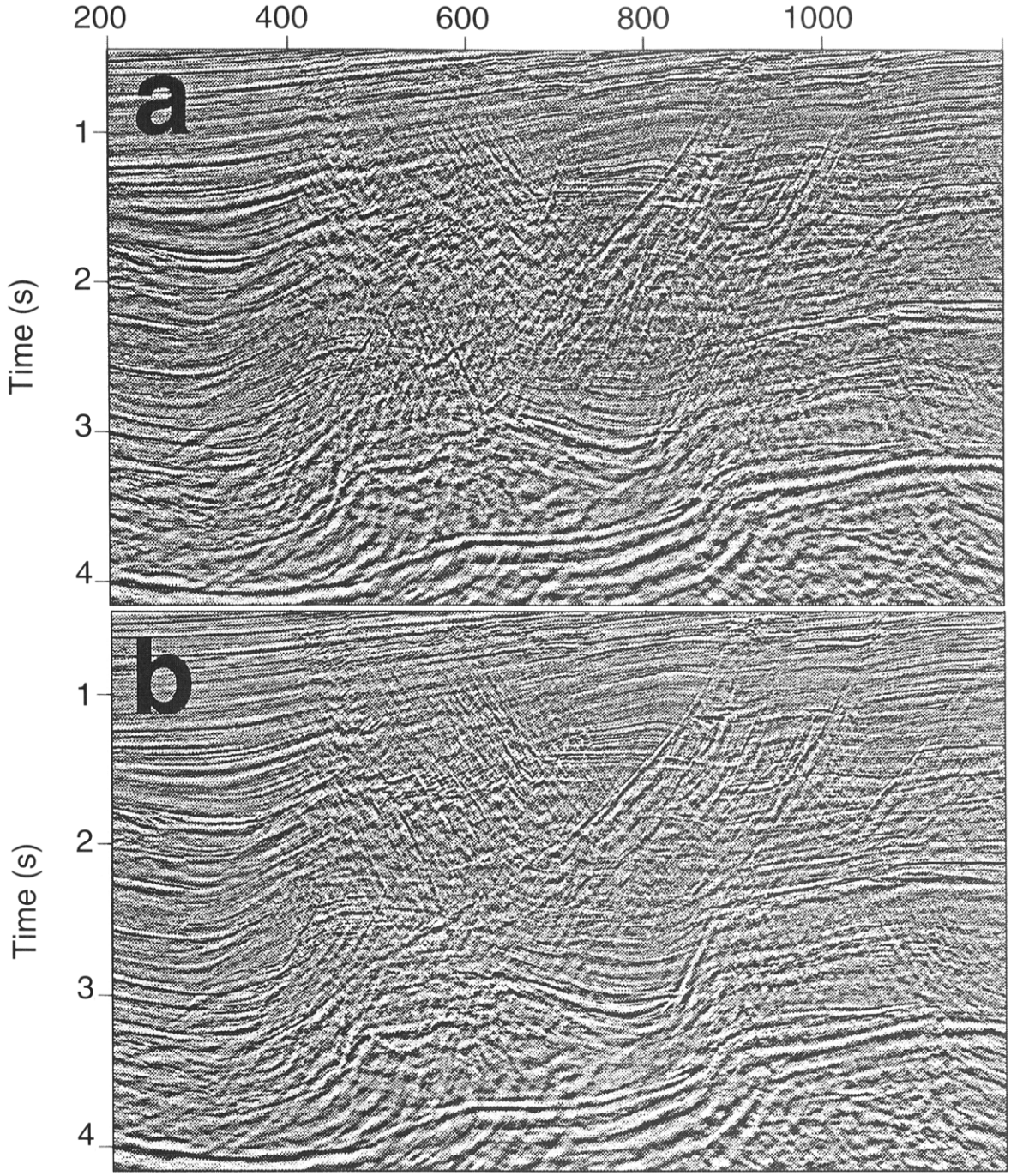

Figure 10. Comparison between the results of isotropic and anisotropic 2-D processing. (a) section obtained by isotropic phase-shift migration. (b) anisotropic phase-shift migration using the parameters shown in Figure 9.

haps, the stretched DMO helped to focus the fault-plane reflections, and artificially high velocities may have been used in the time migration to compensate for the presence of anisotropy. Such use of higher velocities may be helpful if the locations of the dipping events are known in advance, such as where the positions of fault-plane reflections are supported by the reflections from bedding. The artificially high velocities, however, seem to have caused overmigration of interfaces at depth. For instance, the image of the bottom reflection under CMP location 900 in Figure 8 looks overmigrated.

Discussion and conclusions. Despite the clear improvements achieved by the anisotropic imaging methods, it may be thought that accounting for anisotropy in processing is too costly. However, although anisotropic DMO and migration codes are somewhat more complicated algorithmically than their isotropic counterparts. they are often almost as efficient in terms of computing time and memory requirements. For instance, the TZO algorithm used in our work is based on traveltime tables calculated once for any model and is, therefore, as fast as the corresponding isotropic algorithm. In migration codes that make repeated use of ray tracing, the overall cost of adding anisotropy depends on the contribution of ray tracing to the total computing time (this contribution is small, for example, for Gaussian beam migration).

Hence, the main message of this work is that it is *no longer justified* to apply isotropic imaging methods in the

presence of vertical transverse isotropy, even if adjustments of the processing parameters can bring about local improvements in image quality. Processing that takes anisotropy into account is neither too complex nor too costly, nor is anisotropy in the earth's subsurface unusual. Rather the opposite: it is *isotropy* that is anomalous in the earth.

To an extent, routine processing (devised for isotropic media) often includes some freedom, e.g., a juggling of velocities, that allows the processor to overcome some limitations imposed by ignoring the true presence of anisotropy. With such freedom, the processed result can often be steered toward a "geologically plausible" solution, although with only limited success for the offshore Africa data. Despite all attempts to artificially adjust the parameters of the isotropic processing flow, it failed to image fault planes in a massive shale formation. It should be emphasized that the strength of the anisotropy (in time imaging, measured by the parameter η) in this study area was not anomalous, and similar results can be expected in other regions (e.g., in the North Sea). Also, with the advent of prestack depth migration instead of the conventional processing sequence of NMO-DMO-poststack migration, the possibilities of turning knobs on isotropic algorithms become much more limited.

It might be thought that the added parameter η, here, accomplishes little more than the benefit of having an added degree of freedom in processing. We should emphasize, however, that for the offshore Africa data, the same function $\eta(\tau)$ obtained from the inversion of dip-moveout data yielded not only an improved stack of the dipping events after DMO but also improved migrated position and improved nonhyperbolic moveout correction of the gently dipping features.

Furthermore, the significant improvement in image quality represents just one of the benefits of accounting for transverse isotropy in seismic processing. Another benefit, that may be equally important, is the possibility of obtaining a new physical parameter of the subsurface (η) from P-wave reflection data. This coefficient has the potential of becoming an important tool in lithology discrimination from surface seismic data, even if an acceptable image could have been obtained without applying anisotropic processing. For instance, in the Gulf of Mexico the influence of transverse isotropy on DMO is counteracted by a vertical velocity gradient (Lynn et al., 1991), which enables the isotropic NMO-DMO-poststack migration sequence (with some "adjustments" of velocity) to image fault-plane reflections. However, even in this case, η may serve as a useful lithologic tool that would allow the interpreter to discriminate between shales and sands using only surface data. LE

Acknowledgements: We thank the partnership of Sonangol, Chevron, Elf and Agip for donating the field data used in this paper and the students (T. Galikeev, H. Jaramillo, A. Ruger) of the "A(nisotropy)-Team" within the Center for Wave Phenomena (CWP) at the Colorado School of Mines. We wish to acknowledge financial support by the members of the Consortium Project on Seismic Inverse Methods for Complex Structures within CWP and by the Department of Energy (project "Velocity Analysis, Parameter Estimation, and Constraints on Lithology for Transversely Isotropic Sediments" within the framework of the Advanced Computational Technology Initiative).

References

Alkhalifah, T. 1995, Anisotropy processing in vertically inhomogeneous media: Center for Wave Phenomena, Colorado School of Mines (CWP- 162).

Alkhalifah, T. 1995, Transformation to zero offset in transversely isotropic media: GEOPHYSICS, in print.

Alkhalifah, T., and Tsvankin, I., 1996, Velocity analysis for transversely isotropic media, GEOPHYSICS, **60,** 1550-1566.

Ball, G., 1995, Estimation of anisotropy and anisotropic 3-D prestack migration, offshore Zaire, GEOPHYSICS, **60,** 1495-1523.

Crampin, S., 1985, Evidence for aligned cracks in the earth's crust: First Break, **60,** no. 3, 12-15.

Lynn, W., Gonzalez, A., and MacKay, S., 199 1, Where are the fault-plane reflections?: 61st Annual International Mtg., SEG, Expanded Abstracts, 1151-l 154.

Thomsen, L., 1986, Weak elastic anisotropy: GEOPHYSICS, **51,** 1954-1966.

Tsvankin, I., 1995, Normal moveout from dipping reflectors in anisotropic media: GEOPHYSICS, **60,** 268-284.

Tsvankin, I., 1996, P-wave signatures and notation for transversely isotropic media; An overview: GEOPHYSICS; **61,** 467-483.

Tsvankin, I., and Thomsen, L., 1994, Nonhyperbolic reflection moveout in anisotropic media: GEOPHYSICS, **59,** 1290-1304.